ELSEVIER

Polymer 41 (2000) 121–131

polymer

Melting behavior and identification of polymorphic crystals in syndiotactic polystyrene

R.H. Lin[a,*], E.M. Woo[b]

[a]*Department of Chemical Engineering, National Kaohsiung Institute of Technology, Kaohsiung, 80782 Taiwan*
[b]*Department of Chemical Engineering, National Cheng Kung University, Tainan, 70101 Taiwan*

Received 15 July 1998; received in revised form 4 January 1999; accepted 9 January 1999

Abstract

Melting peaks and resulted crystal forms in syndiotactic polystyrene (s-PS) subjected to various thermal treatments were thoroughly investigated using DSC and X-ray diffraction. This study concluded that the four major crystal forms were individually generated and no transformation occurred between α', α'', β' and β'' forms during thermal treatments. Thickening of these crystals, however, was likely during either slower heating scan (i.e. dynamic annealing) or extended isothermal annealing at relatively high temperatures. Different polymorphs were found to dominate the observed multiple melting endotherms of a thermally treated s-PS sample, which was erased of the thermal history in advance. Through cross-reference between the thermograms and X-ray crystallographs, each of the multiple melting peaks in DSC thermograms of s-PS was individually assigned and associated with the identified crystal forms. The melting peak of β-form is always located at lower temperature than those of α-form. Meanwhile, β-form is less thermally stable than α-form.

Keywords: Syndiotactic polystyrene (s-PS); Multiple melting behavior; Dynamic annealing

1. Introduction

The polymorphic behavior of syndiotactic polystyrene (s-PS) is very complex. In the past, substantial works in structure studies have been carried out using X-ray diffraction [1–11], Fourier transform infrared spectroscopy (FTIR) [12–17], solid-state nuclear magnetic resonance (NMR) [18,19], Raman spectrum [20,21] and electron diffraction [22]. Four different crystalline forms have been described so far, and termed as α, β, γ and δ [1]. The crystalline α and β forms are characterized by chains in the *trans* planar conformation, whereas the crystalline γ and δ forms have chains in the s(2/1)2 helical conformation. The crystalline δ form has been used to indicate different clathrate structure (compounds which include molecules of solvent) or emptied clathrate form (δ_e) [10,17].

A typical, thermally processed s-PS sample usually exhibits only two main types of crystals α (α' and α'') and β (β' and β''). Therefore, we focus our attention on these two types of crystal. Both α and β forms can probably exist in different modifications having different degrees of structure order, so two limiting disordered modifications (α' and β') and two limiting ordered modifications ($\alpha''$and β'') have been described [1,3,4]. Guerra et al. [1] have demonstrated that no β-form to α-form transition happens during the heating. But, α-form can transform to β-form when annealed at higher pressures [23]. Besides the four crystalline forms, two mesomorphic modifications have been also described [6,24].

The crystal structure of α [3,9,11,22] and β [4,7] forms have been further determined. Greis et al. [22] suggested a model with three triplets (nine chains) packed in a trigonal unit cell for α'' modification and with a one-triplet trigonal unit cell for α' modification. In the model of De Rosa [9], α'' modification is a trigonal quasi-rhombohedral symmetry with three triplets of chains packed and α' modification is a statistical rhombohedral symmetry. The model proposed by De Rosa for α-form is different from that proposed by Gries et al., because of a rotation of 30° and the rhombohedral shift along z of the triplet of chains.

De Rosa et al. [4] also proposed a statistical structure model for β-form. The regular successive stacking of macromolecular bilayers AB–AB gives rise to the ordered β'' modification, and the disordered β' modification is characterized by a defect in stacking with pairs of bilayers of the kind AA or BB. They have also demonstrated that no β' to β'' transition occurs during the re-crystallization of the β'

* Corresponding author. Tel.: + 886-7-7403496; fax: + 886-7-7459386.
E-mail address: rongh@ms19.hinet.net (R.H. Lin)

0032-3861/00/$ - see front matter
PII: S0032-3861(99)00127-5

modification in the melting region. Tsuji et al. [25,26] suggested a model that the disordered β' modification is due to stacking faults that take place in stacking alternatively two types of motif, whereas the ordered β'' modification corresponds to the perfectly regular stacking.

Wide-angle X-ray diffraction patterns [1,4,9] (WAXD) were used to identify the isolated α', α'', β' and β'' crystal forms. The typical β' form peaks are present at $2\theta = 6.1$, 10.4, 12.3, 13.6, 18.6, 20.2, 21.3, 23.9 and 24.9°. Two additional peaks are at $2\theta = 11.8$ and 15.8°, which characterize the β'' form. The typical α' form peaks are found at $2\theta =$ 6.7, 11.8, 13.5 and 20.1°; α'' presents four additional peaks at $2\theta = 10.3$, 14.0, 15.6 and 18.0°. Neat α'' and β' modifications can be individually obtained from γ-form powder (solution-cast) [1]. Neat β'' modification was obtained by casting from an *o*-dichlorobenzene solution at 170°C and neat α' was obtained from δ-form under suitable conditions [1].

There have been substantial studies on the multiple melting behavior of PEEK [27–31], poly(butylene terephthalate) (PBT) [32,33], poly(1,4-phenylene sulfide) (PPS) [34,35], and other semicrystalline polymers. The interpretations vary from reorganization model [36] to dual-morphology model [37] or even polymorphic behavior.

There are few of studies dealing with the melting behavior of s-PS. In the DSC melting behavior, only one melting peak was observed for α'' modification in various scanning rates [1]. The increase in the melting temperature by the reduction of the heating rate suggested the occurrence of reorganization behavior for isolated α'' modification [1].

However, triple melting peaks are usually observed in a DSC thermogram at a scanning rate of 10°C/min for a thermally treated s-PS sample that was erased of the thermal history by melting as-received sample to 300°C and followed immediately by cooling the sample to room temperature by the moderate cooling rate in the range 2–20°C/min. It is believed that different polymorphs may dominate the observed triple melting endotherm, but no one so far has provided a direct evidence for assigning the melting peaks to specified crystalline forms or modifications. The lower and higher melting endothermic peaks of α-form shifted to merge together as a higher annealing temperature was used. In this case, whether α' to α'' transition occurs? In addition, two preceding peaks far above the original melting peak were generally found in the DSC scan at 10°C/min of the bulk s-PS specimen if annealed at a higher temperature above the original melting temperature. What modification should be responsible for that respective peak?

The goals of the present article are: (1) to provide comprehensive thermal and X-ray diffraction evidence to explain the observed melting behavior; (2) to assign the multiple melting peak to the corresponding crystalline forms or modifications; and (3) to investigate whether mutual transformation occurs between α' and α'' modifications, and incidentally to recheck any transformations as mentioned in the literature [1,4] (α to β, and β' to β'') by methods different from those that they have used.

2. Experimental

2.1. Materials and sample preparation

The s-PS ($M_w = 2.41 \times 10^5$ and $M_w/M_n = 2.31$) was supplied by Idemitsu Petrochemical Co. (Japan). As-received s-PS was first melted to erase the thermal history and then subjected to various prescribed thermal treatments, described in detail in Section 3. All crystallization and thermal treatments of s-PS were performed in the cell of the differential scanning calorimeter, therefore the temperature accuracy and control for annealing or crystallization of the polymer samples were excellent.

2.2. Differential scanning calorimetry (DSC)

A differential scanning calorimeter (Perkin-Elmer DSC-7) was used for various thermal treatments (quenching, annealing, or melt-crystallization) of the samples and to observe the melting endothermic peaks. The temperature and enthalpy were calibrated with high-purity indium and zinc standards. A stream of nitrogen at a flow rate of 20 ml/min was used to purge the DSC cell. Relatively small sample sizes (4–5 mg) were used to minimize the effect of thermal conductivity of polymers. Melting peaks were determined by a scanning rate of 10 °C/min from ambient temperature, unless otherwise stated. In thermal treatments of sample, the fastest programmed cooling rate (−300°C/min) was used for quenching the samples; whereas the actual temperature was kept up with the programmed cooling rate only in the early stage (ca. above 250°C), thereafter lagged behind the programmed cooling rate. Therefore, this quenching procedure may not lead to amorphous sample.

2.3. Wide-angle X-ray diffraction (WAXD)

The X-ray instrument used for room temperature diffraction was DIANO 8536 with copper Kα radiation. For elevated temperature diffraction, SIEMENS Diffractometer D5000 with copper Kα radiation was used with a roughly controlled heating rate and a purged nitrogen gas. Specimens s-PS used in X-ray diffractometer were prepared in DSC with various thermal treatments or crystallization by methods similar to those described for the thermal analysis. From the patterns of the diffractometer, the percent contents of the two crystalline forms present in the thermal-treated sample were quantitatively evaluated from characteristic peaks at $2\theta = 11.8$ and 12.3° by an approximate relation [1].

3. Results and discussion

A lot of samples were prepared in the DSC cell through this study. To avoid ambiguity and for brevity, we

Table 1
Summary of the prescribed thermal treatment for various samples

	Sample code	Descriptions about thermal treatment
A series (neat α-form)	A1	As-received sample was heated to 300°C to melt crystal with 10°C/min, then cooled immediately to room temperature with the programmed cooling rate of 300°C/min.
	A11, A12, A13, A14	Sample A1 was treated initially with a heating rate of 10°C/min from room temperature to 263°C, then followed by a heating rate of 0.1°C/min from 263 to 274°C (A11), 263 to 276°C (A12), 263 to 278°C (A13) and 263 to 280°C (A14), respectively, and finally cooled immediately to room temperature by the programmed cooling rate.
B series (neat β-form)	B1	As-received sample was heated to 290°C to melt crystal with 30°C/min, then cooled immediately to 255°C with the cooled rate of 10°C/min, and crystallized at 255°C for 30 min, and finally cooled to room temperature with the programmed cooling rate of 300°C/min.
	B11, B12, B13, B14	Sample B1 was treated initially with a heating rate of 10°C/min from room temperature to 263°C, then followed by a heating rate of 0.1°C/min from 263 to 270°C (B11), 263 to 274°C (B12), 263 to 276°C (B13) and 263 to 278°C (B14), respectively, and finally cooled immediately to room temperature by the programmed cooling rate.
C seires (bulk specimen)	C10	As-received sample was heated to 340°C and held at this temperature for 1 min, then cooled to 250°C with the programmed cooling rate of 300°C/min and crystallized at 250°C for 30 min, and last cooled again to room temperature with the programmed cooling rate of 300°C/min.
	C11, C12, C13, C14, C15	As-received sample was heated to 300°C and held at this temperature for 1 min, then quenched to 245°C with the programmed cooling rate of 300°C/min and crystallized at 245°C for 10 min (C11), 30 min (C12), 60 min (C13), 150 min (C14) and 300 min (C15), respectively, and finally cooled again to room temperature with the programmed cooling rate of 300°C/min.
	C16	s-PS specimen was heated to 300°C to melt crystal, then cooled to room temperature at 10°C/min, subsequently re-heated to 263°C with a rate of 10°C/min again, then followed by a heating rate of 0.1°C/min from 263 to 276°C, and finally quenched immediately to room temperature by the programmed cooling rate.

summarize the prescribed thermal treatments for the most of samples in Table 1. Sample A1 was prepared to generate a neat α-form of s-PS, whereas samples A11, A12, A13 and A14 were made from sample A1 via special thermal treatment. Sample B1 was of the neat β-form and samples B11, B12, B13 and B14 were produced by treating sample B1. Sample C series contains both α and β forms prepared by specified thermal treatments.

In our analysis, melting behavior and X-ray identification of the neat α-form (sample A series) and the β-form (sample B series) generated from the bulk s-PS specimen were first investigated separately, and then the melting peaks and crystallographs of the polymorphic s-PS (sample C series) were finally analyzed to identify a possible correlation.

3.1. Characterization of the α-form of s-PS

3.1.1. Identification of melting peaks for α' and α'' modifications

X-ray diffraction pattern of sample A1, shown in Fig. 1A(a), suggests that only α-form (may include α' and α'') was found. For direct comparison, Fig. 1B(a) shows the corresponding DSC thermogram of this sample at a scanning rate of 10°C/min, exhibiting two main endothermic peaks at 265 and 270.8°C. Whereas, Guerra et al. [1] have shown that substantially the same melting behavior was observed for the α'' modification either transformed from the γ or δ form, or melt-crystallized by various cooling rates. Only one melting endotherm always close to 270°C was measured at the scanning rate of 10°C/min. [1]. (The same behavior will also be observed by following our experiments.) Therefore, the lower peak (265°C) in Fig. 1B(a) was reasonably inferred to be of the α' and could be reasonably attributed to a slightly less ordered form.

3.1.2. Isothermal annealing effect on melting peaks and crystal transition of α-form

X-ray diffraction patterns were obtained for the following samples that were prepared by heating sample A1 at 10°C/min to annealing temperature of 264, 267 and 270°C for 10 min, respectively, and subsequently cooling the annealed sample to room temperature with the programmed cooling rate of 300°C/min. The patterns of these samples remained unchanged as that of sample A1 except that, the increase in the relative intensity near 20.2°, indicating that all of these annealed samples contain both α' and α'' modifications as sample A1 and the percent content of α'' modifications (relative area of characteristic peaks at $2\theta = 10.3$, 14.0 and 15.6°) is unchanged even after annealed at any given higher temperature. This result also implies that no $\alpha' - \alpha''$ mutual transition occurs during annealing at a higher temperature. A representative pattern is shown in Fig. 1A(d) for the sample that was annealed at 270°C for 10 min.

The corresponding DSC thermograms of these annealed samples, shown in Fig. 1B(b), 1B(c) and 1B(d), illustrate that the melting peaks of α' and α'' forms shifted simultaneously to a higher temperature and became closer as annealing temperature increased. Because no α' to α'' transition occurrs, these observations can be only interpreted that original main lamellae of crystal could be increasingly reorganized or/and thickened by the ascending annealing

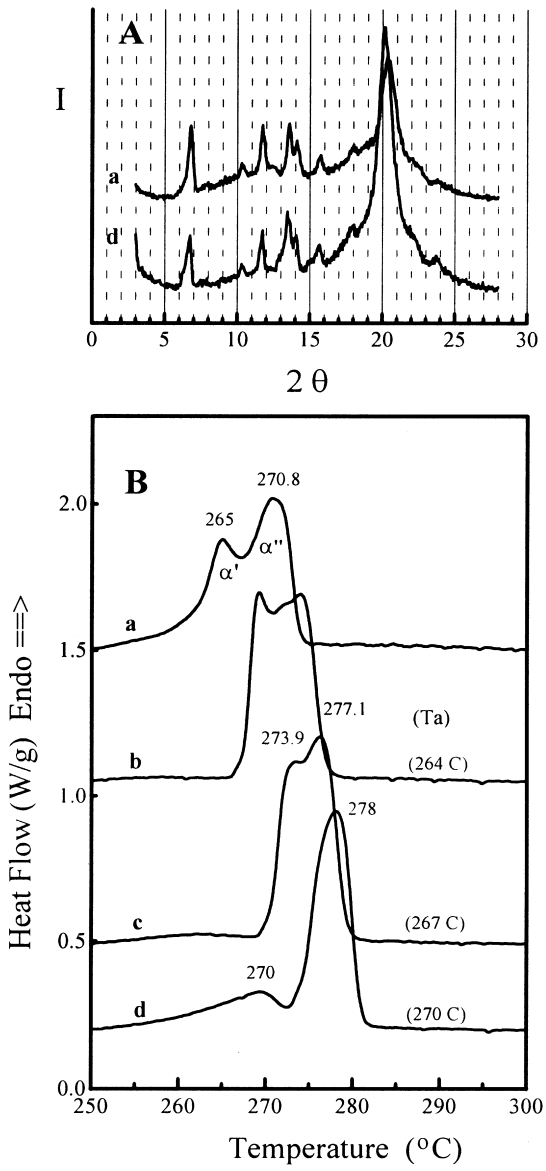

Fig. 1. A. Representative X-ray diffraction patterns of samples related to the DSC thermograms (a) and (d) in B. B. DSC heating scans (10°C/min) of sample A1 (a), and the samples post-treated by annealing A1 at the following temperature for 10 min (b) 264, (c) 267, and (d) 270°C, respectively.

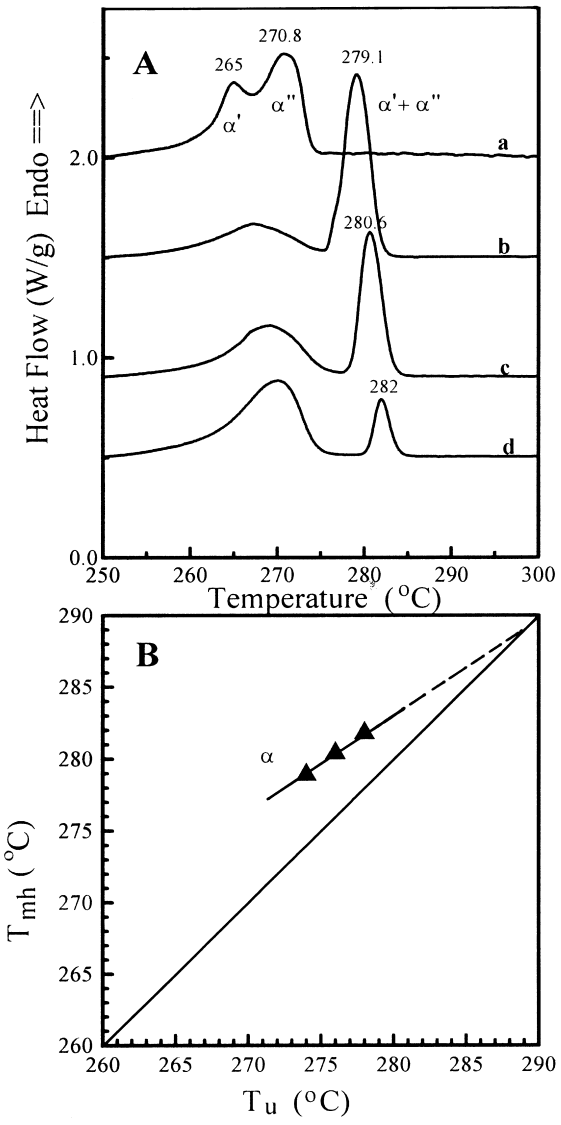

Fig. 2. A. Comparisons of the DSC thermograms of sample A1 (a) and those subsequently subjected to the treatment of different dynamic-annealing range: (b) sample A11, 263–274°C; (c) sample A12, 263–276°C; (d) sample A13, 263–278°C. B. Melting temperature of high-temperature peak for α-form, T_{mh}, as functions of the temperature of the upper limit of dynamic-annealing range, T_u.

temperatures. The degree of shifting for α' modification is larger than that for the α'' modification, probably because the α' modification is originally less ordered and hence more feasible to reorganize and thicken. But, the α' structure is never transformed to α'' structure even if α' modification is reorganized to a more perfect form. Fig. 1B(d) shows that two main endothermic peaks of α' and α'' modifications proceeded eventually to merge together at 278°C when a higher annealing temperature of 270°C was applied. Thereafter, the merged peak will progressively proceed to a higher temperature without peak separation when a higher annealing temperature than 270°C was applied. In addition to this merged peak, a broader minor peak at 270°C was observed due to the melting of thin crystals which were produced by the fastest programmed cooling from the molten parts of a relatively thinner lamellae at an annealing temperature of 270°C. For a full assessment of the situation, the whole thermogram should be presented from room temperature to 300°C. Actually, the baseline from room temperature to 250°C is a straight line without any change. For clearly illustrating the necessary part of the curves, only a narrower temperature range (250–300°C) of DSC thermograms are presented (the same situation for all the subsequent DSC thermograms in the following sections). In summary, the observations from DSC and X-ray results demonstrated that during the slower heating scan or in annealing process at an elevated temperature no α'–α'' mutual transition occurs

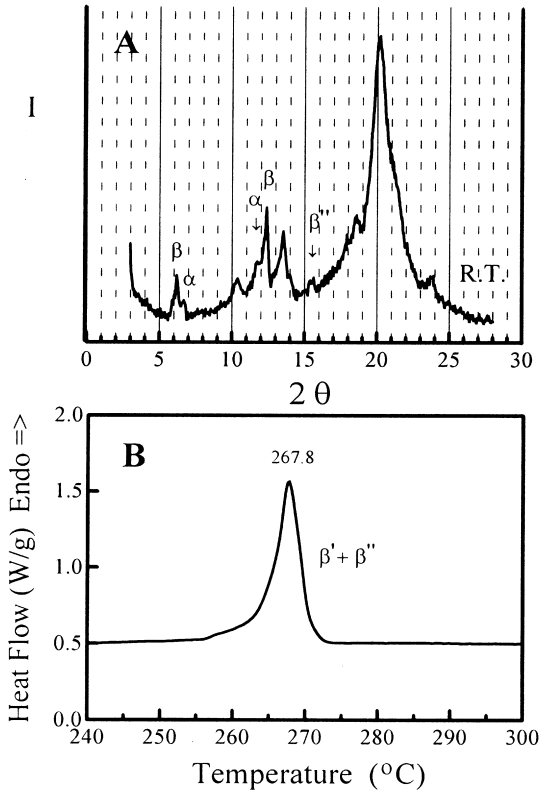

Fig. 3. A. X-ray diffraction pattern of sample B1. B. The DSC thermogram of sample B1.

but only a thickening of the respective form of lamellae occur.

3.1.3. Effect of dynamic scan on melting peaks and crystal transition of the α-form

DSC scan was performed at 10°C/min for sample A1 that was held 3 min at the following sequence of progressively ascending temperatures during the heating, 262, 264, 266, 268, 270, 272 and 274°C. Only one merged melt peak was observed shifting to 279.1°C during the whole process. Actually, procedure described above can exert the same effect as annealing. Obviously, melting of original main lamellae in the α-form is not a prerequisite for forming a thicker lamellae by recrystallization and remelting at a higher temperature. A similar procedure was performed in X-ray scan, the holding time of 3 min was just for X-ray to finish the scan. X-ray diffraction patterns showed no change for each step (including at room temperature step, A1). All of them concluded as α' and α'' forms. Although there is an uncertainty as to the exact heating rate used for diffraction work, the trend of these diffraction patterns associated with the corresponding DSC thermograms, however, is without loss of coincidence. No α'–α'' mutual transition occurs during the heating scan and this was again justified from this observation of unchanged relative peak area in X-ray diffraction patterns.

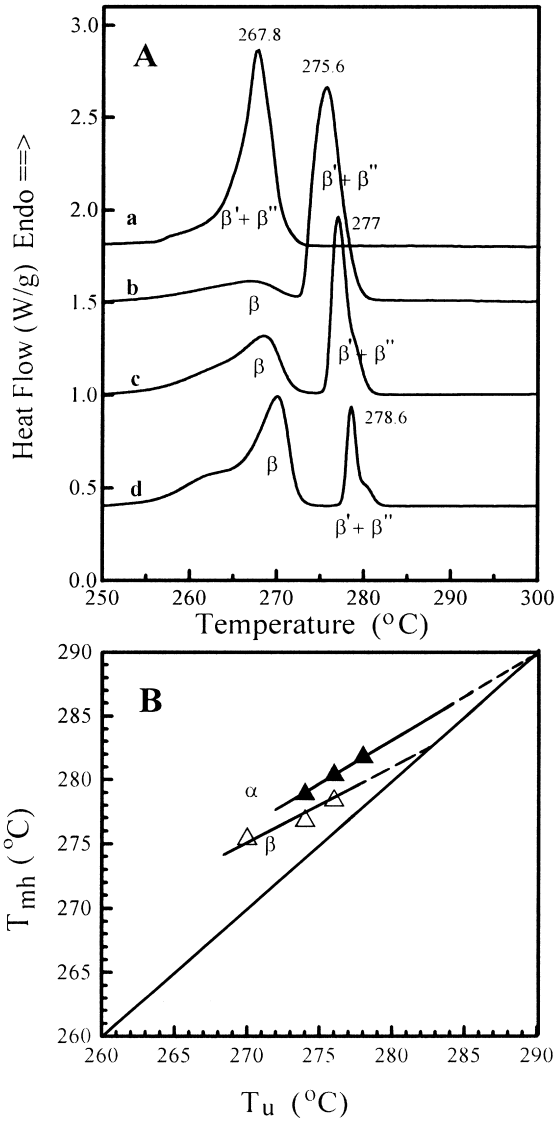

Fig. 4. A. Comparisons of the DSC thermograms of sample B1 (a) and those subsequently subjected to the treatment of different dynamic-annealing range: (b) sample B11, 263–270°C; (c) sample B12, 263–274°C; (d) sample B13, 263–276°C. B. Comparison of melting temperature of high-temperature peak, T_{mh}, of the β-form (empty symbols) and the α-form (solid symbols), as functions of the temperature of the upper limit of dynamic-annealing range, T_u.

3.1.4. Effect of dynamic-annealing on melting peaks and crystal transition of α-form

To investigate the melting behavior of the bulk s-PS specimen when a rather slow heating rate was performed, we prepared the samples A11–A14 and B11–B14 in advance, which were for the individual neat α-form and β-form studies, respectively. Curves a, b, c and d in Fig. 2A show the DSC scan at 10°C/min of samples A1, A11, A12 and A13, respectively. A significantly higher melting peaks were found at 279.1, 280.6 and 282°C for A11, A12 and A13, respectively, suggesting that the slower heating rate (0.1°C/min) allowed sufficient time for some extra chain segments to fold and form thicker main lamellae.

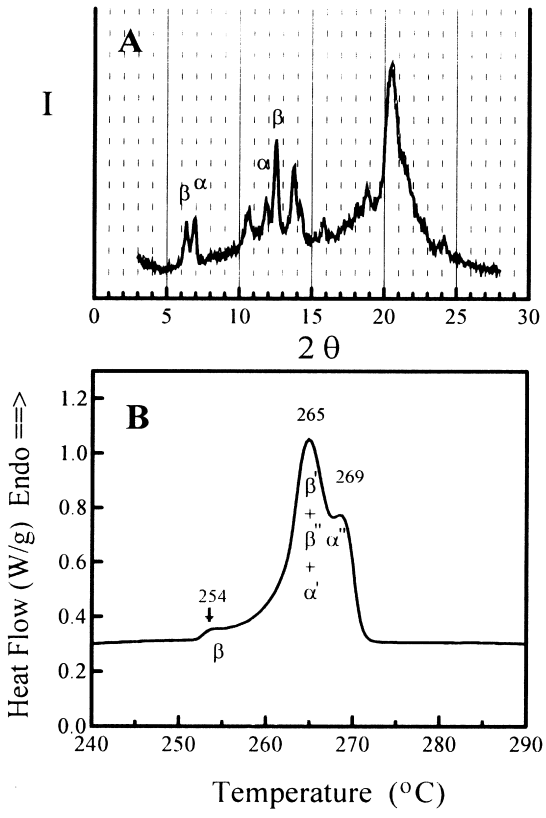

Fig. 5. A. X-ray diffraction pattern of sample C10. B. The corresponding DSC heating scan (10°C/min).

The procedure with a very slow heating rate (such as 0.1°C/min here) within a higher temperature range is temporarily referred to as the 'dynamic-annealing' here. The area of higher melting peak gradually diminished as the upper limit of dynamic-annealing range increased, indicating that more and more polymer chain segments cannot fold and form more thicker lamellae at a higher dynamic-annealing temperature.

Higher melting peak were 5, 4.6 and 4°C above the upper limit of the dynamic-annealing range for A11 (263–274°C), A12 (263–276°C) and A13 (263–278°C), respectively, revealing that the degree of shifting of higher melting peak continuously decreased as the upper limit of dynamic-annealing temperature increased. These results were represented in Fig. 2B, in which T_u represents the temperature of the upper limit of dynamic-annealing range and T_{mh} is the melting temperature of the high-temperature peak being shifted due to dynamic-annealing. It is believed that the area and melting temperature of the shifting peak will increase to a limit with the decrease in the heating rate of dynamic-annealing, because there is sufficient time for chain segments to fold and form more thicker main lamellae. Theoretical maximum value of equilibrium melting temperature for α-form was determined to be 289°C from Fig. 2B.

X-ray diffraction patterns of these three treated samples (A11, A12 and A13) and the original sample (A1) were

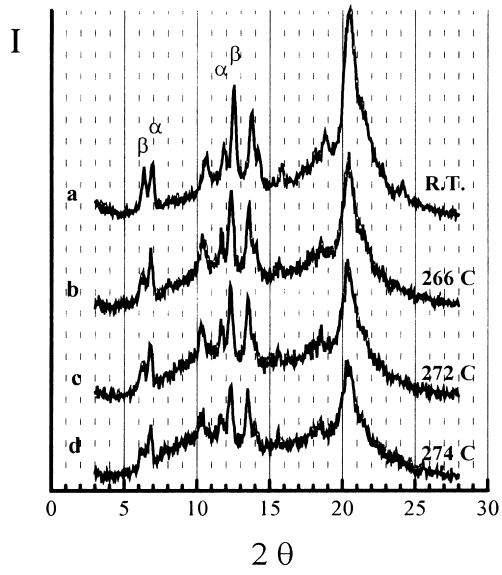

Fig. 6. X-ray diffraction patterns of sample C10 during the heating (a) at room temperature, and at following temperatures: (b) 266, (c) 272, and (d) 274, in which sample C10 was subsequently held for 3 min at the following sequence of progressively ascending temperature during heating, 262, 264, 266, 270, 272 and 274°C.

virtually the same, comprising α′ and α″ modifications. Accordingly, it can be reasonably predicted from previous observations that the higher melting peak was mutually contributed by α′ and α″ crystals. Incidentally, the lower broad melting peak in each DSC thermogram resulted from the melting of thin crystals which were produced by the fastest programmed cooling rate from the molten part of relatively thinner lamellae at a higher dynamic-annealing temperature. The thin crystal produced above was still in the α-form (the fastest programmed cooling process have been proved to lead the exclusive formation of α-form crystal irrespective of the maximum melt temperature and the holding time at that temperature).

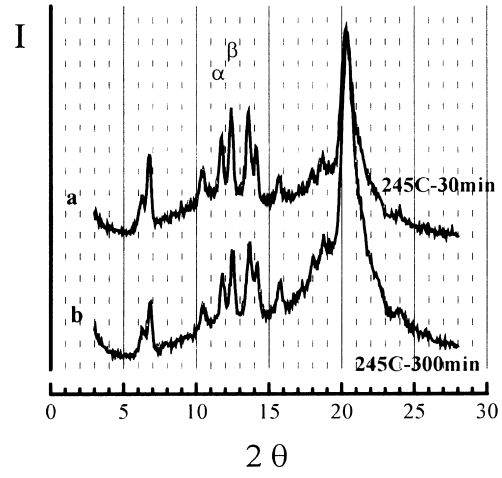

Fig. 7. X-ray diffraction patterns of samples C12 (a) and C15 (b), these samples were melt-crystallized at 245°C for 30 and 300 min, respectively.

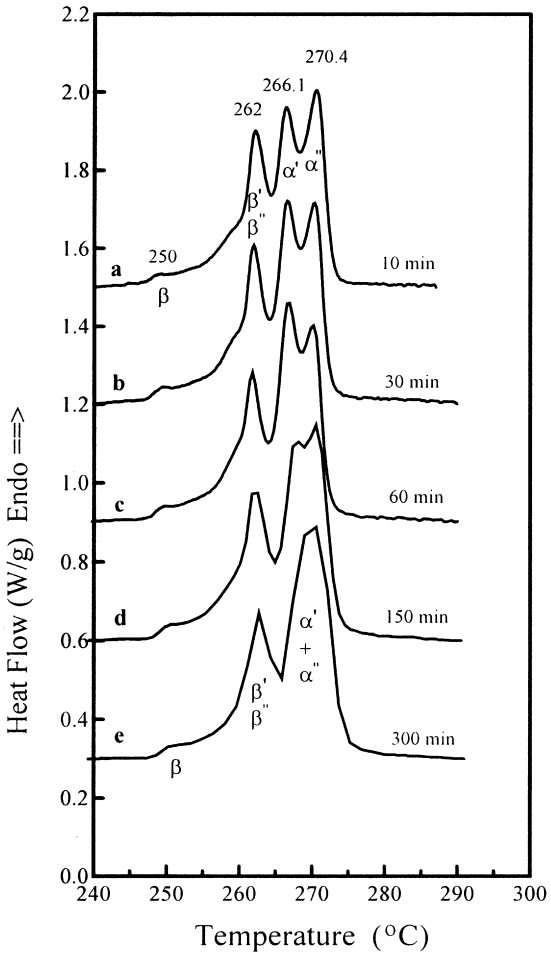

Fig. 8. DSC heating scans (10°C/min) of samples C11 (a), C12 (b), C13 (c), C14 (d) and C15 (e). These samples were melt-crystallized at 245°C for 10, 30, 60, 150, and 300 min, respectively.

3.2. Characterization of the β-form of s-PS

3.2.1. Identification of melting peaks for β′ and β″ modifications

From the X-ray diffraction pattern of the sample B1, shown in Fig. 3A, the percent content of the β-form crystal (containing β′ and β″) was above 90%, which was evaluated from the characteristic peaks at $2\theta = 11.8$ (α-form) and 12.3° (β-form) by an approximate relation [1]. The percent content of the β-form produced in this way was large enough for us to examine the melting behavior. Fig. 3B shows the DSC thermogram of sample B1 at a scanning rate of 10°C/min. Although sample B1 is composed of β′ and β″ modifications (characteristic peaks for β″ is at $2\theta =$ 15.8°), only one endothermic peak was observed at 267.8°C due to the isothermal crystallization process at 255°C for 30 min.

3.2.2. Effect of dynamic scan on melting peaks and crystal transition of the β-form

DSC scanning was performed at 10°C/min for sample B1 that was held for 3 min during heating in a sequence of progressively ascending temperatures of 262, 264, 266, 268, 270 and 272°C. Original melt peak was found to shift to 275.6°C due to original main lamellae in the β-form being continuously thickened without remelting and recrystallization which is the same behavior as that of the α-form. A parallel procedure was performed in the X-ray scan and the holding time of 3 min was for the X-ray scan. X-ray diffraction patterns exhibited no change for each step (including at room temperature step, B1). Results of DSC thermogram associated with X-ray diffraction patterns suggested that the melting peak at 275.6°C was mutually contributed by the β′ and β″ crystals. Apparently, no β′–β″ mutual transition occurred during the heating from the observations of unchanged relative peak area in X-ray diffraction patterns. Rosa and coworker [4] have proved that no β′ to β″ mutual transformation can occur from their observations.

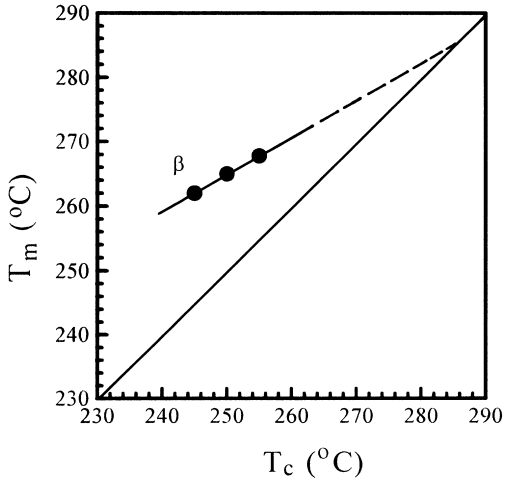

Fig. 9. Melting temperature of the β-form, T_m, as functions of melt-crystallization temperature T_c.

3.2.3. Effect of dynamic-annealing on melting peaks and crystal transition of β-form

The method of dynamic-annealing used to treat the α-form crystal was again applied to treat the β-form crystal for comparison. Curves (a), (b), (c) and (d) in Fig. 4A show the DSC scan at 10°C/min of samples B1, B11, B12 and B13, respectively. Peaks of significant shifting were found at 275.6, 277 and 278.6°C for B11, B12 and B13, respectively. The melting peaks for β′ and β″ were always lumped together to successively proceed to a higher melting temperature without changing any situation of macromolecular bilayer stacking. The area of higher melting peak diminished as the temperature of the upper limit of dynamic-annealing range increased, manifesting itself the same behavior as the α-form in folding some extra chain segments into main lamellae.

Higher melting peaks were 5.6, 3 and 2.6°C above the upper limit of the dynamic-annealing range for B11 (263–270°C),

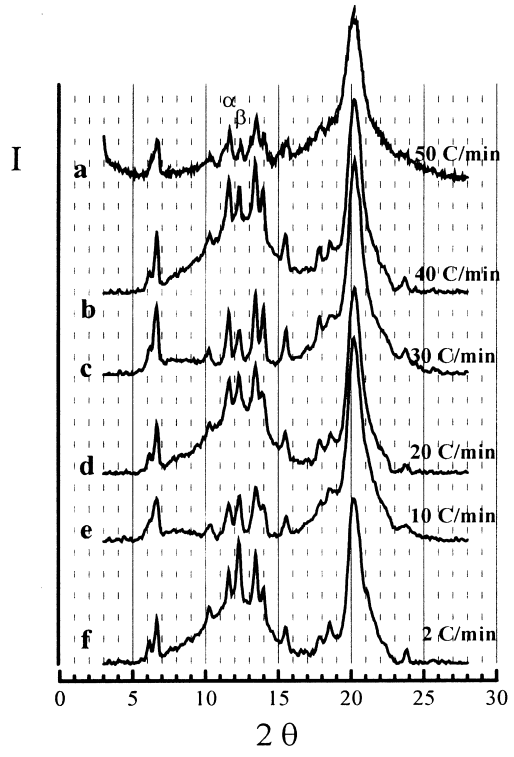

Fig. 10. X-ray diffraction patterns of various samples that were cooled from melt state with the following rates: (a) 50, (b) 40, (c) 30, (d) 20, (e) 10, and (f) 2°C/min.

B12 (263–274°C) and B13 (263–276°C), respectively, presenting a significantly smaller temperature difference $T_{mh} - T_u$ than that of the α-form. Thus, it demonstrated that the shifting melting peaks were indeed resulted from β-form crystal and mutually contributed by the β′ and β″ modifications. These results were represented as empty symbols in Fig. 4B and compared with those of the α-form (solid symbols) from Fig. 2B. Theoretical maximum value of equilibrium melting temperature for β-form was estimated to be 283°C, lower than that of the α-form.

The same X-ray diffraction patterns of the four samples (original B1, and treated B11, B12 and B13) elucidated that the compositions of crystal-form did not have any change that comprised of the β′ and β″-form crystals and a small amount of α-form crystal. These results demonstrated again that no β′–β″ mutual transition occurred during the dynamic-annealing at a higher temperature. By the way, the lower broad melting peak in each DSC thermogram resulted from the melting of thin crystals which were produced by the fastest programmed cooling rate from the molten parts of thinner lamellae at higher dynamic-annealing temperature. The majority of these thin crystals were identified as the β-form from X-ray diffraction patterns. In contrast to this, however, a fastest programmed cooling from melt state generally produces α-form crystals only. This indicates that existence of nuclei of the β-form (β′ or β″) in the melt state led to the β-form crystals preferably generated. Additionally, sample B14 was prepared by applying dynamic-annealing range from 263 to 278°C, resulting in the disappearance of the preceding peak in DSC thermogram, whereas the preceding peak still remained at 282°C for α-form using the same dynamic-annealing range.

3.3. Melting behavior of s-PS specimen with α and β crystals

3.3.1. Assignment of melting peaks for specimen containing α and β crystals

From the X-ray diffraction pattern of the sample C10, shown in Fig. 5A, the percent content of the β-form crystal was much larger than that of the α-form crystal. Fig. 5B shows the DSC thermogram of sample C10 at a scanning rate of 10°C/min. Two main endothermic peaks were observed at 265 and 269°C in which the peak area of the lower temperature was overwhelmingly larger than that of the higher temperature. It follows that the melting peak of lower temperature (265°C) was dominantly contributed by the β-form crystal which is a much larger amount. Meanwhile, the melting peak of higher temperature (269°C) was by no means contributed by the β-form produced by isothermal crystallization at 250°C for 30 min, because the melting temperature was no more than 267.8°C for the β-form that was produced by isothermal crystallization even at 255°C for the same length of time (sample B1, described in Fig. 3B). More briefly, the melting peak obtained by the lower crystallization temperature never exceeded that obtained by higher crystallization temperature. Although the β′ and β″ crystals coexisted in sample C10, only one endothermic peak was observed at 265°C due to the crystallization process at 250°C for 30 min. This is consistent with the observation of the DSC thermogram of sample B1, in which only one endothermic peak was observed for β′ and β″ crystals. Meanwhile, the α′ and α″ crystals contributed their due fraction to a lower temperature peak and a higher temperature peak, respectively. This is consistent to the observation of the DSC thermogram as illustrated in the sample A1, in which the two melting peaks were produced by the fastest programmed cooling rate and annealing process at 250°C for 30 min. Another smaller minor peak (indicated by arrow) was found at 254°C, which was presented by the β-form due to the annealing effect at 250°C for 30 min. All assignments of peaks are summarily indicated in Fig. 5B.

3.3.2. Stability for each crystal-form

To examine the thermal stability, we dynamically performed X-ray scan of the sample C10 at a heating rate of 10°C/min. During the heating from room temperature, the sample C10 was held 3 min at the following sequence of progressively ascending temperature, 262, 264, 266, 270, 272 and 274°C, and performed an X-ray scan within that holding time. For brevity, only three sets of X-ray diffraction patterns are presented in Fig. 6 to compare the

polymorphic change with the original sample C10 (curve (a), at room temperature state). We found that the relative amount of the β-form crystal ($2\theta = 6.1$ and 12.3°) continuously decreased as the scan temperature increased. There may be two reasons. First, the β-form has less thermal stability at the elevated temperature. Second, the transition occurs from β-form to α-form at the elevated temperature. Actually, no transition from β-from to α-form occurs and will be demonstrated in the following paragraph.

3.3.3. Effect of crystallization time on melting peaks and crystal transition of the bulk s-PS

Irrespective of the crystallization time, unchanged X-ray diffraction patterns of all samples C11, C12, C13, C14 and C15 (representing two patterns in Fig. 7) indicated that no α–β mutual transition occurred for samples subjected to isothermal crystallization at the elevated temperature. This result via X-ray diffraction method matched the DSC observation of Guerra et al. [1].

Curves (a)–(e) in Fig. 8 show the corresponding DSC thermograms of crystallized samples C11, C12, C13, C14 and C15, respectively. Three main peaks were observed at 262, 266.5 and 270.4°C in thermogram (a). The middle peak and the highest peak were supposed to be α' and α'' modifications, respectively, as explained previously. From the observation, middle peak (α') shifted gradually to a higher temperature and eventually merged in the highest peak (α'') without transition from α' to α'' but only lamellae reorganization and thickening of α' as the crystallization time increased. The lowest peak (262°C) was supposed to be cooperatively contributed by β' and β'' modifications, because this interpretation coincided with the trend of $T_m - T_c$ relationship, shown in Fig. 9. Solid symbols of this figure are the melting temperature of β' and β''modifications at 267.8, 265 and 262°C for samples B1, C10 and C12 crystallized at 255, 250 and 245°C, respectively, for 30 min. There is no discernible shifting for the lowest and highest peak regardless of the increase in the crystallization time unless a higher annealing temperature is used. Effect of crystallization time on lamellae thickening in α'' and β forms is less than the effect of the higher annealing temperature on that. In addition to three main peaks, one smaller minor peak was also observed at 250°C, which was presented by the β-form due to the annealing effect at 245°C.

3.3.4. Effect of cooling rate on melting behavior and the formation of polymorphs

To explore this subject, we prepared some samples with different cooling rate from melt state. Curves (a)–(f) in Fig. 10 show the X-ray diffraction patterns of samples that were heated to 300°C to melt crystal, then cooled to room temperature with the following rates: 50, 40, 30, 20, 10 and 2°C/min, respectively. It suggests that β-form crystal ($2\theta = 12.3°$) significantly increased as the cooling rate decreased. The β-form is favored at the lower cooling rate

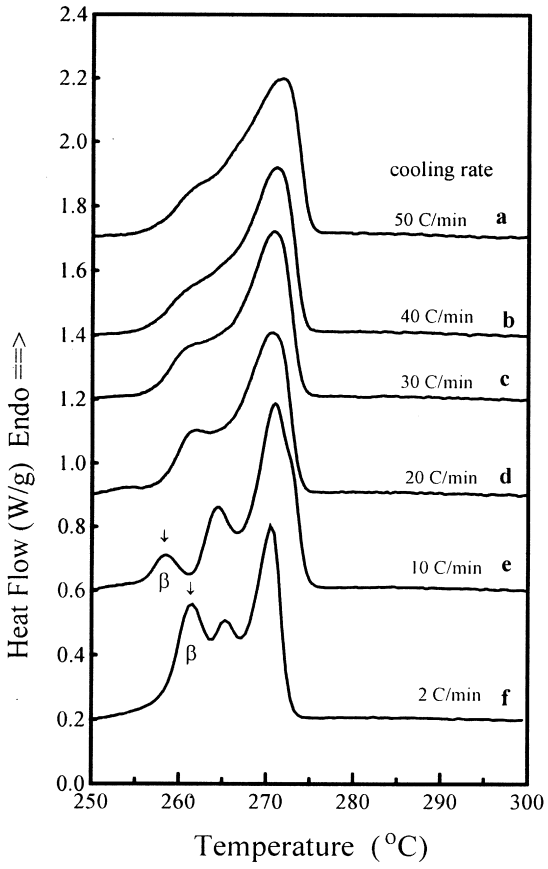

Fig. 11. DSC heating scans (10°C/min) of various samples that were cooled from melt state with the following rates: (a) 50, (b) 40, (c) 30, (d) 20, (e) 10, and (f) 2°C/min, the corresponding X-ray diffraction patterns are shown in Fig. 10.

because it needs more time to fold the chain segment and thicken the lamellae, whereas the α-form is favored at a faster cooling rate in the absence of external pressure. The corresponding DSC thermograms at 10°C/min are shown in Fig. 11, exhibiting the change of peaks from two broader to three sharper peaks. It implied that the peaks of lower temperature indicated by arrows were supposed to be of the β-form. It can be concluded that the melting peaks of β-form are always lower than those of α-form when the same thermal treatment was taken. Furthermore, it indicates that the β-form had less thermal stability under the same condition.

3.3.5. Effect of dynamic-annealing on melting peaks and crystal transition of the bulk s-PS

Two preceding peaks far above the original melting peak were generally found in the DSC scan at 10°C/min of s-PS specimen containing both α-form and β-form if annealed at a higher temperature above original melting temperature. We wanted to know why two preceding peaks instead of one were formed and what polymorphs were assigned to those peaks. Therefore, the dynamic-annealing method is used as an example to illuminate the phenomena observed.

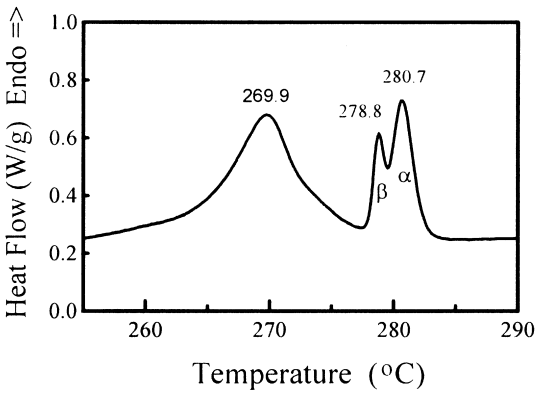

Fig. 12. DSC heating scan (10°C/min) of sample C16 subjected to the dynamic-annealing from 263 to 276°C.

The sample C16 was prepared for this subject. Fig. 12 shows the DSC scan at 10°C/min of the sample C16, in which two preceding peaks far above the original melting peak were found at 278.8 and 280.7°C which were exactly the same as observed in the β-form (shown earlier in Fig. 4A(d)) and the α-form (shown earlier in Fig. 2A(c)), respectively, for the same thermal treatment and dynamic-annealing range. It is apparent that the higher and the lower one of the two preceding peaks were contributed by the α-form and the β-form, respectively. It follows from the earlier observations that the melting peak of β-form is always lower than that of the α-form. The specimen s-PS that contains both α-form and β-form is a prerequisite for the formation of the two preceding peaks.

Doublet minor peaks below the original melting peak were also found in the DSC scan at 10°C/min of s-PS specimen containing both the α-form and β-form which was annealed at a lower annealing temperature below original melting temperature. Predictably, doublet minor peaks were contributed by α-form and β-form, respectively, and followed that the melting peaks of β-form are always lower than those of the α-form. This will be further discussed in future work.

4. Conclusions

In general, double or triple melting peaks are usually observed within the temperature range of 255–275°C for a thermally processed s-PS specimen in DSC heating scan. In the doublet-peaks case, if the s-PS specimen contains both α-form and β-form, then the lower peak of DSC thermogram is supposed to be associated with β', β'' and α', and the higher peak is with α''. If the s-PS sample is known to contain the α-form only, then the lower peak is supposed to be associated with α' crystal, and the higher peak should be with α''. In triple-melting peaks case, s-PS specimen always contains both α-form and β-form, and hence the lowest temperature peak is suggested to be due to $\beta'$and β'', the middle peak is α' and the highest temperature peak should be due to α''. When a higher annealing temperature (above 270°C) or a longer annealing time is applied, the α' peak will shift gradually to merge into the α'' peak without transition from α' to α'', whereas β' and β'' are always assigned to the same peak and are always lower than the α-form peak.

Samples containing α-form and β-form were treated by special dynamic-annealing process, correspondingly, doublet peaks far above the original melting peak were always observed. The lower temperature peak was mutually due to the β' and β'', whereas the higher temperature peak was mutually contributed by the α' and α''. No transformation between α', α'', β' and β'' occurs but only a thickening of lamellae in each crystals occur either during the slower heating scan or annealing at high temperatures.

Acknowledgements

This work was financially supported by the National Science Council, under contract number NSC 88-2216-E-151-003. Thanks are also extended to Mr. Masahiko Kuramoto of Idemitsu Petrochemical Co., Ltd. (Japan) and Prof. E.M. Woo of National Cheng Kung University (Taiwan) for the supplying the s-PS specimen. Acknowledgment is due to Prof. E.M. Woo for his review of the manuscript.

References

[1] Guerra G, Vitagliano VM, De Rosa C, Petraccone V, Corradini P. Macromolecules 1990;23:1539.
[2] Guerra G, De Rosa C, Vitagliano VM, Petraccone V, Corradini P. J Polym Sci Polym Phys Ed 1991;29:265.
[3] De Rosa C, Guerra G, Petraccone V, Corradini P. Polym J 1991;23:1435.
[4] De Rosa C, Rapacciuolo M, Guerra G, Petraccone V, Corradini P. Polymer 1992;33:1423.
[5] Chatani Y, Shimane Y, Inone Y, Inagaki T, Ishhioka T, Ijitsu T, Yukinari T. Polymer 1992;33:488.
[6] Auriemma F, Petraccone V, Dal Poggetto F, De Rosa C, Guerra G, Manfredi C, Corradini P. Macromolecules 1993;26:3772.
[7] Chatani Y, Shimane Y, Ijitsu T, Yukinari T. Polymer 1993;34:1625.
[8] Manfredi C, Guerra G, De Rosa C, Busico V, Corradini P. Macromolecules 1995;28:6508.
[9] De Rosa C. Macromolecules 1996;29:8460.
[10] De Rosa C, Guerra G, Petraccone V, Pirozzi B. Macromolecules 1997;30:4147.
[11] Cartier L, Okihara T, Lotz B. Macromolecules 1998;31:3303.
[12] Reynolds NM, Savage JD, Hsu SL. Macromolecules 1989;22:2867.
[13] Kobayashi M, Nakaoki T, Ishihara N. Macromolecules 1990;23:78.
[14] Reynolds NM, Hsu SL. Macromolecules 1990;23:3463.
[15] Reynolds NM, Stidham HD, Hsu SL. Macromolecules 1991;24:315.
[16] Musto P, Tavone S, Guerra G, De Rosa C. J Polym Sci Polym Phys Ed 1997;35:1055.
[17] Guerra G, Manfredi C, Musto P, Tavone S. Macromolecules 1998;31:1329.
[18] Capitani D, Segre AL, Grassi A, Sykora S. Macromolecules 1991;24:623.
[19] Capitani D, De Rosa C, Ferrando A, Grassi A, Segre AL. Macromolecules 1992;25:3874.
[20] Kellar EJC, Galiotis C, Andrews EH. Macromolecules 1996;29:3515.

[21] Kellar EJC, Evans AM, Knowles J, Galiotis C, Andrews EH. Macromolecules 1997;30:2400.
[22] Greis O, Xu Y, Asano T, Peterman J. Polymer 1989;30:590.
[23] Sun Z, Morgan RJ, Lewis DN. Polymer 1992;33:660.
[24] Manfredi C, De Rosa C, Guerra G, Rapacciuolo M, Auriemma F, Corradini P. Macromol Chem Phys 1995;196:2795.
[25] Tsuji M, Okihara T, Tosaka M, Kawaguchi A, Katayama K. MSA Bull 1993;23:57.
[26] Tosaka M, Hamada N, Tsuji M, Kohjiya S. Macromolecules 1997;30:4132.
[27] Blundell DJ. Polymer 1987;28:2248.
[28] Lee Y, Porter RS, Lin JS. Macromolecules 1989;22:1756.
[29] Lee Y, Porter RS. Macromolecules 1987;20:1336.
[30] Chang SS. Polym Commun 1988;29:138.
[31] Ko TY, Woo EM. Polymer 1996;37:1167.
[32] Nichols ME, Robertson REJ. Polym Sci, Part B, Polym Phys 1992;30:755.
[33] Kim J, Nichols ME, Robertson RE. J Polym Sci, Part B, Polym Phys 1994;51:57.
[34] Mai K, Zhang M, Zeng H, Qi S. J Appl Polym Sci 1994;51:57.
[35] Huo P, Cebe P. Colloid Polym Sci 1992;270:840.
[36] Blundell DJ, Osborn BN. Polymer 1983;24:953.
[37] Bassett DC, Olley RH, Al-Raheil IAM. Polymer 1988;29:745.